PAPER

Numerical investigation of the stability of stationary solutions in the theory of cathode spots in arcs in vacuum and ambient gas

To cite this article: M S Benilov *et al* 2014 *Plasma Sources Sci. Technol.* **23** 054007

IOP Publishing Plasma Sources Science and Technology

Plasma Sources Sci. Technol. **23** (2014) 054007 (10pp) doi:10.1088/0963-0252/23/5/054007

Numerical investigation of the stability of stationary solutions in the theory of cathode spots in arcs in vacuum and ambient gas

M S Benilov[1], M D Cunha[1], W Hartmann[2] and N Wenzel[2]

[1] Departamento de Física, CCCEE, Universidade da Madeira, Largo do Município, 9000 Funchal, Portugal
[2] Siemens AG, Corporate Technology, Günther-Scharowsky-Strasse 1, 91058 Erlangen, Germany

Received 17 January 2014, revised 2 April 2014
Accepted for publication 15 May 2014
Published 25 September 2014

Abstract

The stability of stationary spots on cathodes of arcs in vacuum and ambient gas is investigated by means of the simulation of the temporal evolution of perturbations imposed over steady-state solutions. Two cases of loading conditions are considered, namely, spots operating at a fixed current (the case typical of small-scale experiments) and spots operating at a fixed voltage (the case typical of high-power circuit breakers). Results are reported on spots on large copper cathodes of vacuum arcs and on spots on tungsten cathodes of high-pressure argon arcs. It is shown, in particular, that if the ballast resistance in small-scale laboratory experiments with a high-current arc is insufficient, the potential consequence may be a thermal explosion of a spot, if the arc burns in vacuum, and massive melting of the cathode surface, if the arc burns in ambient gas. This conclusion conforms to trends observed in the experiment.

Keywords: stability, cathode spots, stationary solutions, arcs in vacuum and ambient gas

S Online supplementary data available from stacks.iop.org/PSST/23/054007/mmedia

(Some figures may appear in colour only in the online journal)

1. Introduction

Considerable advances have been attained in the course of the past 15 years in the theory and modeling of current transfer to cathodes of arcs burning in ambient gases (e.g. [1] and references therein; [2–7] may be cited as further examples). In particular, two- (2D) and three-dimensional (3D) solutions describing, in a self-consistent way, stationary spots on cathodes of arcs in ambient gases can be computed nowadays as a matter of routine with the use of steady-state solvers. Recently, the same approach has been applied to the simulation of stationary spots on cathodes of vacuum arcs [8].

An important issue concerning solutions that describe stationary configurations and have been computed by means of steady-state solvers is their stability under some or other experimental conditions. The stability of different regimes of steady-state current transfer to cathodes of arc discharges, including regimes with spots, was investigated in the framework of the linear stability theory with the use of analytical methods [9] and the eigenvalue solver of the software COMSOL Multiphysics [10]. An alternative approach to the investigation of the stability of stationary solutions is to perturb a stationary solution and then follow the development of the perturbed solution in time by means of a nonstationary solver. This approach, while significantly more demanding in terms of CPU time, allows one to predict the final result of development of perturbations of unstable states.

In this work, the latter approach is applied to the investigation of the stability of stationary solutions describing current transfer, in the first place in the spot mode, to cathodes of arcs burning in vacuum and ambient gas. Two limiting cases of loading conditions are considered, namely, spots operating at a fixed current and spots operating at a fixed voltage; the cases typical of, respectively, low-current arcs and high-current arcs in circuit breakers. The temporal evolution of the perturbed solution is followed until one of the four outcomes

occurs: the perturbation decays, i.e. the spot returns to the original unperturbed state; the local temperature decreases down to the average temperature, i.e. the spot is extinguished; the temperature in the spot rapidly rises to very high values, up to the critical temperature, which can be termed an 'explosion' of the spot; the arc attachment expands and a significant part or the whole of the front surface of the cathode becomes quite hot, which can be termed 'massive melting' of the cathode surface.

The outline of the paper is as follows. The numerical model is briefly introduced in section 2. Results of the numerical investigation of the stability of stationary modes of current transfer to cathodes of arcs in vacuum and ambient gas, performed by means of numerical simulation of the development of perturbations in time imposed over steady-state solutions, are reported in sections 3 and 4, respectively. Conclusions are summarized in section 5.

2. The model

The model of plasma–cathode interaction employed in the above-cited works [2–8] exploits the fact that a significant electric power is deposited by the arc power supply into the near-cathode space-charge sheath. A part of this power is transported from the sheath to the cathode surface and heats up the surface up to temperatures sufficient for thermionic or thermo-field electronic emission. The rest of the deposited power is transported by the electric current into the arc column. As a consequence, the plasma–cathode interaction is, to the first approximation, not affected by processes in the arc column. Note that the arc column is affected by the plasma–cathode interaction through energy flux and electric current from the near-cathode plasma to the arc column.

In order to correctly describe the energy flux from the near-cathode plasma to the surface, one needs to consider, in addition to the near-cathode space-charge sheath, also the ionization layer, which is a thin plasma region adjacent to the sheath where the energy flux to the cathode surface is generated. Since the combined thicknesses of the sheath and the ionization layer are much smaller than a characteristic radius of the arc attachment, current transfer through this region is locally one dimensional (1D). Therefore, the problem of arc–cathode interaction may be solved in two steps. In the first step, a 1D problem of current transfer across the sheath and the ionization layer is solved and characteristics of these zones are found as functions of the local temperature T_w of the cathode surface and of the near-cathode voltage drop U (a combined voltage drop in the sheath and the ionization layer, which is assumed to be the same for all points of the arc attachment). In particular, densities of the net energy flux and the electric current from the plasma to the cathode surface are found: $q = q(T_\mathrm{w}, U)$, $j = j(T_\mathrm{w}, U)$.

In the second step, distributions of temperature T and electrostatic potential φ in the cathode body are calculated by means of solving, in the cathode body, the time-dependent multidimensional heat conduction equation, written with account of Joule heat generation in the cathode body, and the current continuity equation supplemented with Ohm's law:

$$\rho_\mathrm{c} c_p \frac{\partial T}{\partial t} = \nabla \cdot (\kappa \nabla T) + \sigma (\nabla \varphi)^2 , \qquad (1)$$

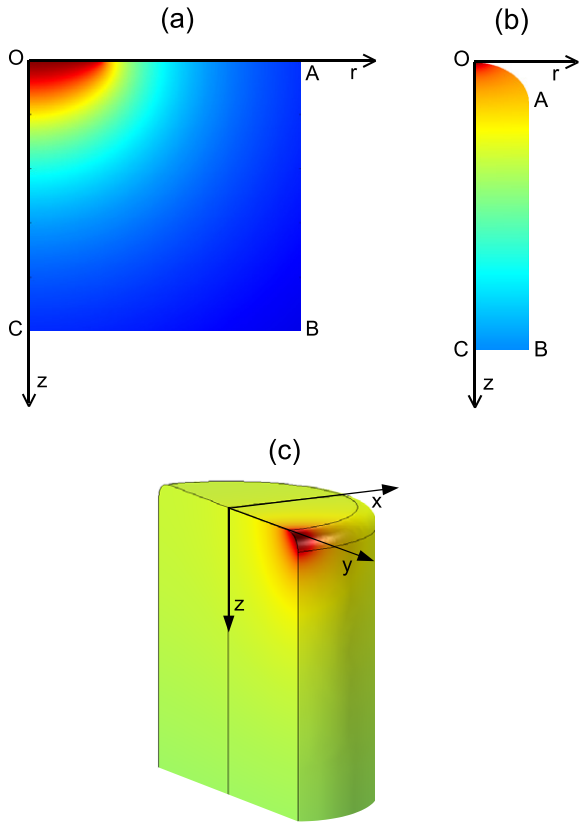

Figure 1. Geometry of the problem. (*a*) 2D spot attached to a planar infinite cathode. (*b*) 2D spot attached to a cylindrical cathode with a hemispherical tip. (*c*) 3D spot attached to a cylindrical cathode with a flat front surface with a rounding at the edge.

$$\nabla \cdot (\sigma \nabla \varphi) = 0. \qquad (2)$$

Here t is time, ρ_c, c_p, κ and σ are, respectively, the mass density, specific heat, and thermal and electrical conductivities of the cathode material. The dependences $q(T_\mathrm{w}, U)$ and $j(T_\mathrm{w}, U)$ calculated in the first step serve as boundary conditions for equations (1) and (2) at the cathode surface:

$$\kappa \frac{\partial T}{\partial n} = q(T_w, U), \qquad \sigma \frac{\partial \varphi}{\partial n} = j(T_w, U), \qquad (3)$$

where n is a direction locally orthogonal to the cathode surface and directed outside the cathode.

Three different geometries shown in figure 1 are considered: an axially symmetric (2D) spot attached to a planar infinite cathode (figure 1(*a*)), a 2D spot attached to a cylindrical cathode with a hemispherical tip (figure 1(*b*)), and a 3D spot attached to a cylindrical cathode with a flat front surface with a rounding at the edge (figure 1(*c*)). In the case of the planar infinite cathode, equations (1) and (2) are solved in 2D in the cylindrical domain designated $OABC$ in figure 1(*a*). Boundary conditions (3) apply on the cathode surface; line OA in figure 1(*a*). Far away from the spot the temperature of the cathode body tends to a given value T_cool (the average temperature of the cathode) and the potential tends to zero. The corresponding boundary conditions on lines AB and BC are implemented as in [8]. In the case of a cylindrical cathode with a hemispherical tip, equations (1) and (2) are

solved in 2D in the domain designated $OABC$ in figure 1(b). Boundary conditions (3) apply on the front and lateral surface of the cathode; line OAB. The base of the cathode (line BC) is assumed to be maintained at a fixed temperature $T_{\rm cool}$ by external cooling and the electrostatic potential here is set equal to zero. The geometry shown in figure 1(c) is similar to that shown in figure 1(b) except that the cathode has a different shape and the spot is 3D.

Results reported in this paper refer to copper cathodes of vacuum arcs and tungsten cathodes of arcs operating in argon. The thermal and electrical conductivities $\kappa(T)$ and $\sigma(T)$ of copper and tungsten were assumed to be the same as in [8] and [6], respectively. The specific heat values $c_p(T)$ of copper and tungsten were evaluated with the use of data from [11] and with account of the latent heat of melting (which was introduced along the same lines as is done in the simulation of metal casting [12]; see [13] for details). Functions $q(T_{\rm w}, U)$, and $j(T_{\rm w}, U)$ were determined as described in [14] for the copper cathodes of vacuum arcs and in [15] for the tungsten cathodes of arcs burning in argon.

The above model neglects the effect of the arc column over cathode spots, which can come into play in some situations, and does not account for convective heat transfer due to motion of molten metal and changes of shape of the cathode surface, which may occur due to motion of molten metal, microexplosions and ejection of macroparticles. Nevertheless, the model has given a number of useful results, also in nonstationary cases (e.g. [13, 16]), and a nonlinear investigation of the stability of stationary solutions describing steady-state spots in the framework of this model seems to be a natural and timely step.

The procedure is as follows. A stationary solution $T = T_0(\boldsymbol{r})$, $\varphi = \varphi_0(\boldsymbol{r})$, $U = U_0$ is computed by means of a steady-state solver for a given value of the spot current, $I = I_0$. Then a perturbation is imposed over this solution and a nonstationary solver is invoked with this perturbed solution being the initial condition. If in the course of temporal evolution the perturbation decays and the system returns to the stationary solution $T_0(\boldsymbol{r})$, $\varphi_0(\boldsymbol{r})$, then the stationary spot described by the solution is stable (against the considered perturbations and for the loading conditions being considered). Otherwise, the spot is unstable and the question is what will happen to it in the course of temporal evolution?

One can consider different forms of the perturbation imposed over the steady-state solution. However, trial calculations have shown that the final outcome stability/instability does not depend on the shape of the perturbation. Most of the results reported in this work refer to perturbations of the distribution of the cathode temperature introduced in the simple form $\beta[T_0(\boldsymbol{r}) - T_{\rm cool}]$, where β is a given parameter characterizing the initial level of perturbation of the cathode temperature, with the distribution of potential being unperturbed. In other words, the initial condition for nonstationary modeling was $T(\boldsymbol{r}) = T_0(\boldsymbol{r}) + \beta[T_0(\boldsymbol{r}) - T_{\rm cool}]$, $\varphi(\boldsymbol{r}) = \varphi_0(\boldsymbol{r})$.

The nonstationary modeling is performed without perturbation of the electric control parameter: it is maintained during the whole simulation run $U = U_0$ or $I = I_0$ in the cases of voltage- and current-controlled spots, respectively. Note that the model of a spot operating at a constant voltage is appropriate for conditions of very high current arcs, such as those in high-power circuit breakers, where many tens or even hundreds of spots operate in parallel and ignition or extinction of a spot does not appreciably affect the arc voltage. The model of a spot operating at a constant current is of interest in connection with moderate-current arc devices and small-scale experiments, where the arc power supply is current-controlled and there is (ideally just) one or a few cathode spots. Note that in both cases of voltage- and current-controlled spots the voltage drop in the near-cathode layer is assumed to be the same at different points of the cathode surface. Distributions along the cathode surface of other parameters, including the density of electric current to the cathode surface, are related to the distribution of temperature of the cathode surface and have to be computed at each time as a part of the solution.

Both steady-state and nonstationary modeling in this work was performed by means of the commercial software COMSOL Multiphysics. The finite-element mesh has to be strongly nonuniform, in particular in the vicinity of the spot edge due to a very fast variation of the density of the energy flux coming from the plasma. A free triangular mesh with several successive refinements in the spot region was used in the 2D geometries shown in figures 1(a) and (b). A free tetrahedral mesh was used for the 3D geometry shown in figure 1(c).

3. Stability of vacuum arc spots

This section is concerned with the results of the investigation of the stability of stationary solutions describing spots on copper cathodes of vacuum arcs. As the first step, we neglect nonuniformities of the cathode surface and assume that the cathode is an infinite half-space. The results reported in this section refer to $T_{\rm cool} = 1200$ K.

Detailed simulations of stationary spots on copper cathodes have been reported in [8]. Here, we only mention that the calculated temperature of a stationary spot (about 4400 K), while being higher than the boiling temperature of copper, is in line with the values given in other works; e.g. [17].

An example of the temporal evolution of perturbations of a voltage-controlled spot is given in figure 2 for four levels of initial perturbations: $\beta = \pm 1\%, \pm 2\%$. The maximum temperature in the cathode body, $T_{\rm max}$, is shown on different scales in figures 2(a) and (b). Also shown in figure 2(b) is the temperature of the cathode surface at the center of the spot, $T_{\rm c}$. Note that in the cases where the initial perturbations of the cathode temperature are negative ($\beta < 0$), the highest temperature in the cathode body at all times is attained on the cathode surface at the center of the spot, so $T_{\rm max} = T_{\rm c}$ and the corresponding lines in figure 2(b) coincide. The spot current is shown in figure 2(c) and the temperature of electrons in the near-cathode plasma layer above the center of the spot in figure 2(d). The horizontal lines in figures 2(a)–(d) represent the steady-state values (or, in other words, values corresponding to the unperturbed state). Note that since the highest temperature in the cathode body in the unperturbed state is attained on the cathode surface at the center of the spot, there is only one horizontal line in figure 2(b).

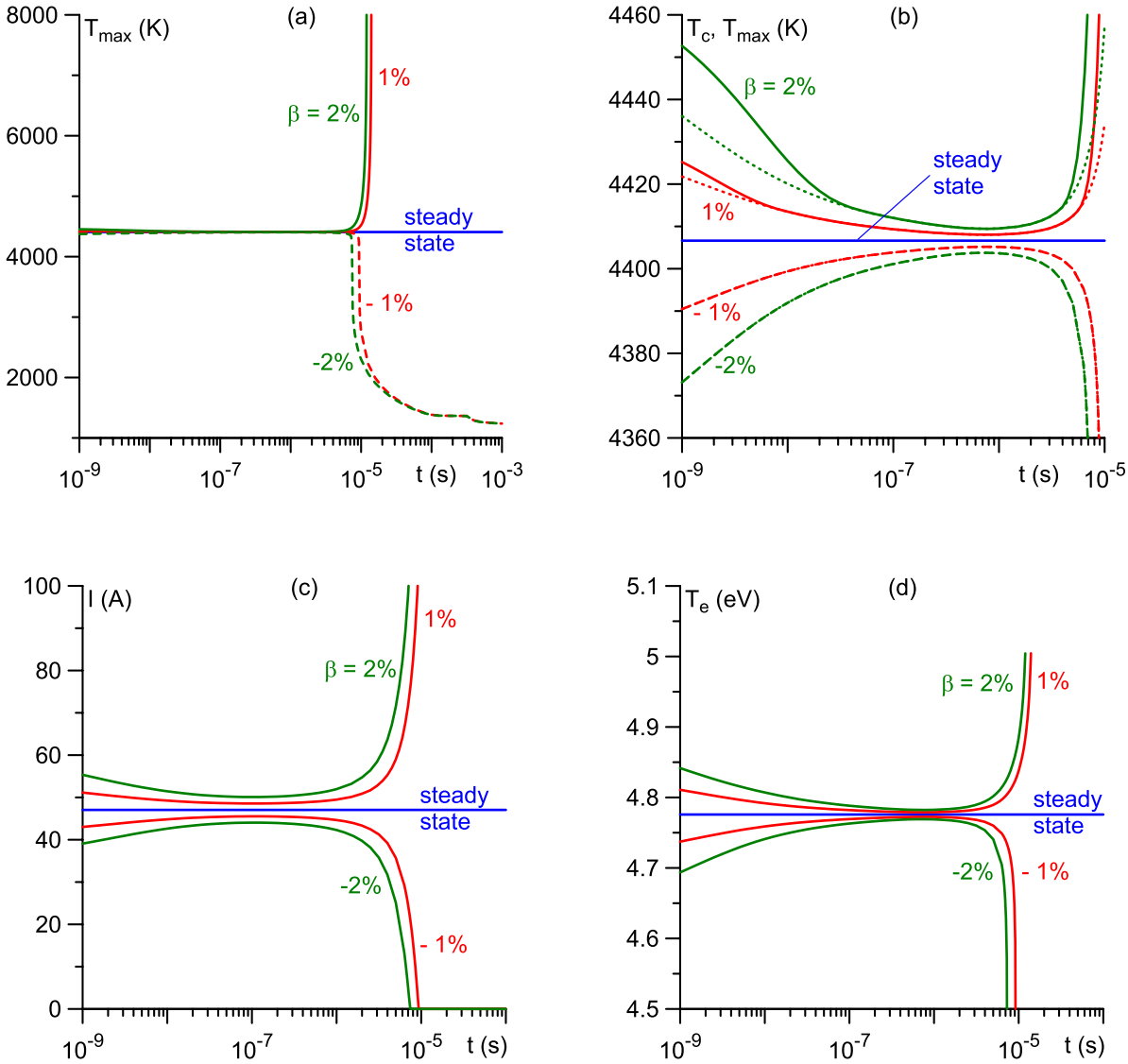

Figure 2. Development of perturbations of a voltage-controlled vacuum spot. $U = 20$ V. (*a*) Maximum temperature in the cathode body, T_{max} (see supplementary data at stacks.iop.org/PSST/23/054007/mmedia). (*b*) T_{max} (solid, dashed) and T_c the temperature of the cathode surface at the center of the spot (dotted). (*c*) Spot current. (*d*) Electron temperature in the near-cathode plasma layer above the center of the spot.

One can see that if the perturbations of the cathode temperature are positive or negative at the initial moment (i.e. β is positive or, respectively, negative), then they remain positive or, respectively, negative at all times. At the first phase, the perturbations decrease on the time scale of nanoseconds, so T_{max} and I approach steady-state values. Note that in the case of positive perturbations ($\beta > 0$) the cathode surface at this phase is cooled down faster than the interior of the cathode, so the temperature maximum is shifted inside the cathode and $T_{max} > T_c$. During some microseconds, T_{max} and I remain close to the stationary values, and the spot radius as well (the corresponding figure is skipped for brevity). At around 10 μs the perturbations start growing once again and rapidly enter the nonlinear phase. In the case of positive perturbations, the temperature maximum is shifted from the surface into the cathode volume and in the course of around one microsecond or less T_{max} and I increase up to extremely high values. One can say that a thermal explosion occurs. In the case of negative perturbations, the spot cools down to temperatures below 2000 K in the course of a few microseconds, after which it continues cooling down at a slower rate and at t of the order of 100 μs T_{max} is virtually indistinguishable from T_{cool}. One can say that the spot is destroyed by thermal conduction.

The same trends are seen in figure 3, which illustrates the temporal evolution of the distribution of the temperature in the cathode body. During some microseconds, the distribution is close to the steady-state one; figure 3(*a*). The temperature maximum which is formed inside the cathode body at the nonlinear phase of development of positive perturbations is localized at a distance of a few μm under the cathode surface; figure 3(*b*).

Thus, stationary solutions describing steady-state spots are unstable if the near-cathode voltage is not affected by processes in a spot. There are two scenarios of the nonlinear

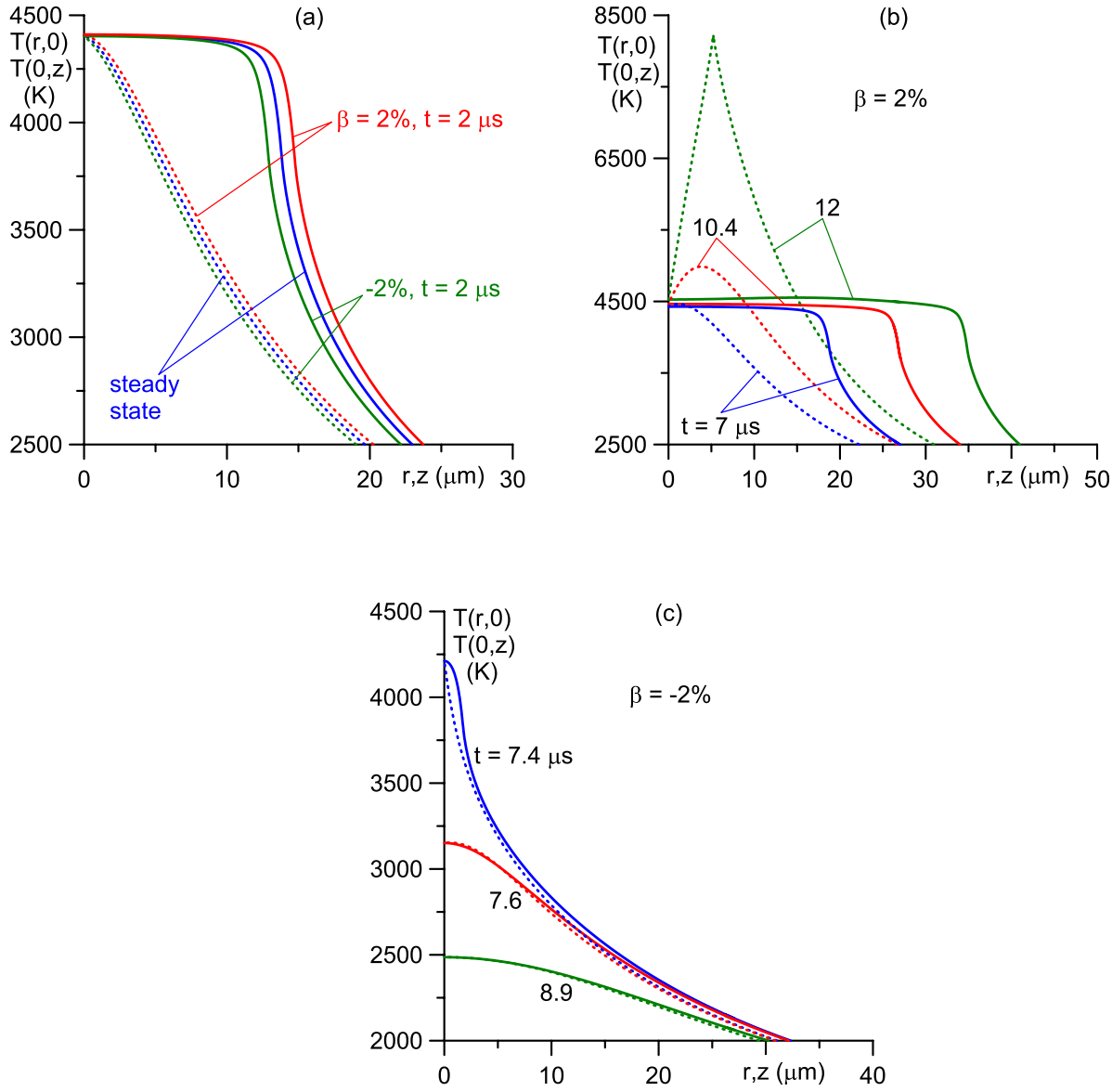

Figure 3. Temporal evolution of distribution of the temperature over the cathode surface (solid) and in the body of the cathode along the axis of symmetry (dotted); voltage-controlled vacuum spot, $U = 20$ V.

development of perturbations: thermal explosion for 'positive' perturbations and destruction of the spot by thermal conduction for 'negative' perturbations.

The characteristic time scales for different variants are given in table 1. Here t_1 represents the time during which the amplitude of the perturbation is reduced to one-half of its initial value; t_2 denotes the time in which the amplitude of the perturbation attains 500 K; and t_3 denotes the time in which the amplitude of the perturbation attains 2000 K. Note that the amplitude of the perturbation here means $|T_{\max} - T_{\max}^{(\mathrm{st})}|$, where $T_{\max} = T_{\max}(t)$ and $T_{\max}^{(\mathrm{st})}$ are the maximum values of the temperature of the cathode body described by, respectively, the perturbed (time-dependent) solution and the stationary solution.

It should be stressed that the modeling reported in this section refers to a semi-infinite cathode with uniform properties and a planar surface. It should be expected that nonuniformities in cathode properties or geometrical

Table 1. t_1: time scale of the initial decay of the perturbation; t_2: time of beginning of the nonlinear phase of the instability; $t_3 - t_2$: time scale of development of the nonlinear phase.

β	t_1(ns)	$t_2(\mu s)$	$t_3 - t_2(\mu s)$
1%	1.6	12.2	1.6
2%	3.7	10.2	1.6
−1%	1.0	9.4	2.3
−2%	1.2	7.5	1.8

nonuniformities of the cathode surface will significantly reduce the time of beginning of the nonlinear phase of development of instability. Therefore, data on t_2 shown in the table may be used as upper estimates and also for qualitative analysis. In particular, one can see that the thermal explosion in the case of positive perturbations begins a little later than the thermal-conduction destruction in the case of negative perturbations. The time of beginning of the nonlinear phase also depends

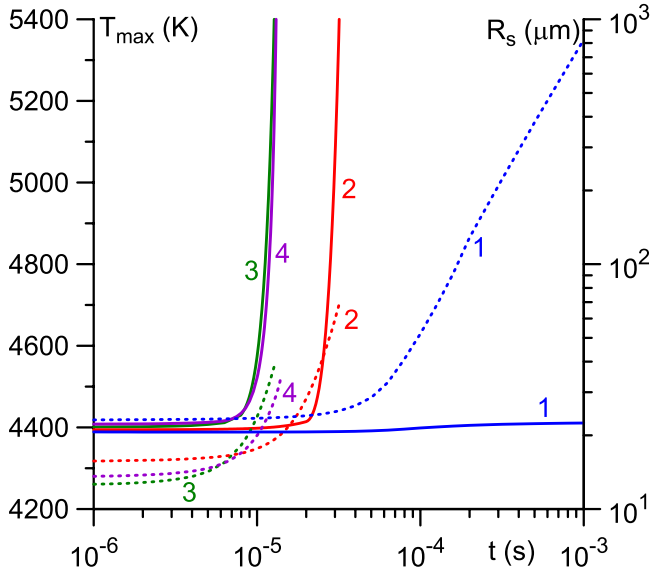

Figure 4. Development of perturbations of a voltage-controlled vacuum spot; $\beta = 1\%$, $U = 20$ V; solid: T_{max}; dotted: spot radius R_s; 1: simulations without account of Joule heating; 2: $\sigma = 3.7 \times 10^6$ S m^{-1}; 3: $\sigma = 1.6 \times 10^6$ S m^{-1}; 4: $\sigma = \sigma(T)$.

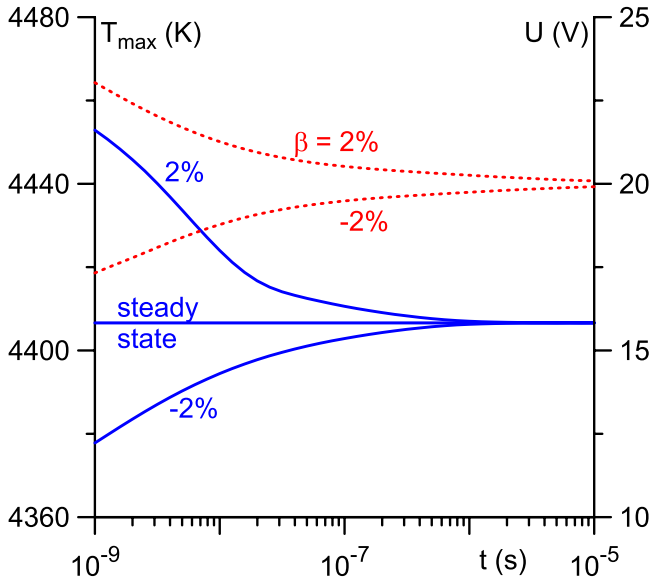

Figure 5. Decay of perturbations of a current-controlled vacuum spot; $I = 47.0$ A; solid: T_{max}; dotted: voltage U.

on the initial level of the perturbation: stronger perturbations enter the nonlinear phase a little earlier, as could be expected.

The above results refer to perturbations which have, at the initial moment, the form $\beta[T_0(\boldsymbol{r}) - T_{cool}]$ with $\beta = \pm 1, \pm 2\%$. However, the same scenarios of development of instability occur also for other perturbations. It is interesting to note that when the initial level of positive perturbations is reduced ($\beta \lesssim 0.5\%$), the maximum of temperature occurs on the cathode surface (i.e. $T_{max} = T_c$) until the perturbation enters the nonlinear phase.

It is clear that the region of very high temperatures underneath the cathode surface that is formed in the course of the nonlinear phase of the development of positive perturbations is a consequence of Joule heat generation in the cathode body. In order to illustrate this relation, the development of positive perturbations of a voltage-controlled vacuum spot computed without account of Joule heating is shown in figure 4 (lines 1). Note that the spot radius plotted in this figure is estimated as the position of a point where the distribution of the density of energy flux from the plasma attains the maximum value; see figure 2b of [8] and its discussion. The spot remains unstable; however, the outcome of the development of perturbations changes: the increase in the maximum temperature (which occurs on the cathode surface) during the nonlinear phase is quite modest, while the spot radius increases to extremely high values. One can say that positive perturbations result in massive melting of the cathode surface in the case where there is no Joule heat generation in the cathode body. Note that negative perturbations result in destruction of the spot by thermal conduction as before.

A question arises as to how important the variability of the conductivity of the cathode material is; one is reminded, in this connection, of the concept of thermal runaway introduced by Hantzsche [18, 19] as an instability caused by a positive feedback between Joule heat production in the cathode body and temperature because of the Wiedemann–Franz law. Lines 2 and 3 in figure 4 depict results of simulations of the development of positive perturbations performed with the electrical conductivity of the cathode material being constant and equal to 3.7×10^6 S m^{-1} or 1.6×10^6 S m^{-1}, which are values of the dependence $\sigma(T)$ for copper at $T = 2000$ K and 4000 K, respectively. For comparison, also shown in figure 4 are data computed for the variable σ; lines 4. (Note that the solid line 4 in figure 4 depicts the same data as the line marked $\beta = 1\%$ in figure 2.) One can see that the development of the instability in the case $\sigma = 1.6 \times 10^6$ S m^{-1} is similar to that in the case of variable σ, although values of the spot radius at the nonlinear phase in the former case are somewhat higher. In the case $\sigma = 3.7 \times 10^6$ S m^{-1} the spot radius at the nonlinear phase is still higher, although still much lower than that in the case of infinitely high σ (i.e. without Joule heating).

One concludes that what affects the development of instability against positive perturbations is not the variability of the conductivity of the cathode material but rather its magnitude.

It is clear that the limitation of the current per spot should produce a stabilizing effect. This is indeed the case, as one can see from figure 5, which refers to the case of the spot current being maintained fixed. Both positive and negative perturbations decrease on the time scale of tens of nanoseconds, so T_{max} and U approach the corresponding steady-state values and remain close to these values ever after. Thus, stationary spots are stable for I fixed. This conclusion conforms to results of the 0D analysis performed in [17, 20], where the spot is described only on the integral level, according to which a steady-state solution can be reached in the course of evolution of a spot at a fixed current.

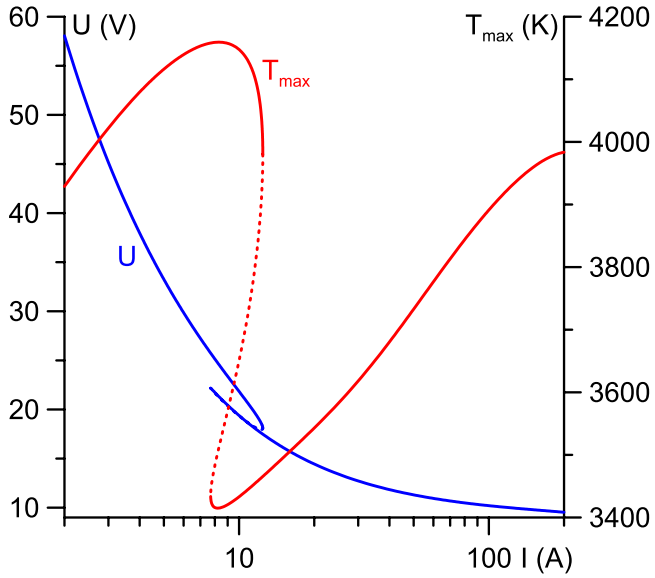

Figure 6. Current–voltage characteristic and maximum temperature of the cathode; $p = 1$ bar, cylindrical cathode with hemispherical tip, $R = 1$ mm, $h = 12$ mm.

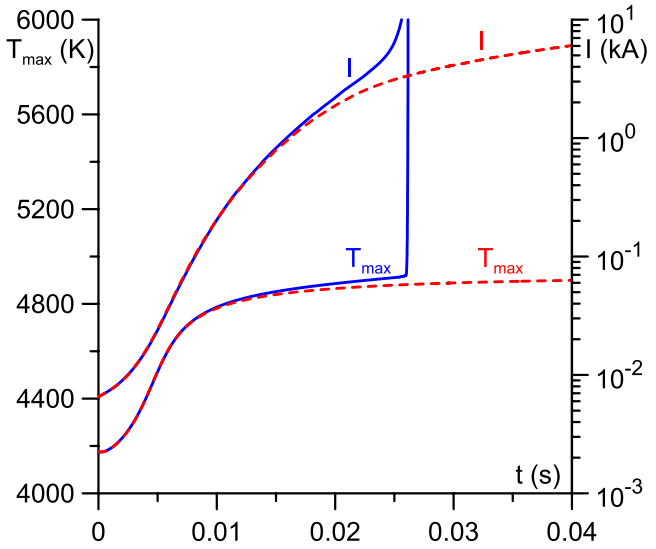

Figure 7. Development of perturbations of voltage-controlled current transfer to cathode of an Ar arc; dashed: simulations without account of Joule heating; $U = 30$ V, $\beta = 1\%$, $p = 1$ bar, cylindrical cathode with hemispherical tip, $R = 1$ mm, $h = 12$ mm. (Supplementary data available at stacks.iop.org/PSST/23/054007/mmedia)

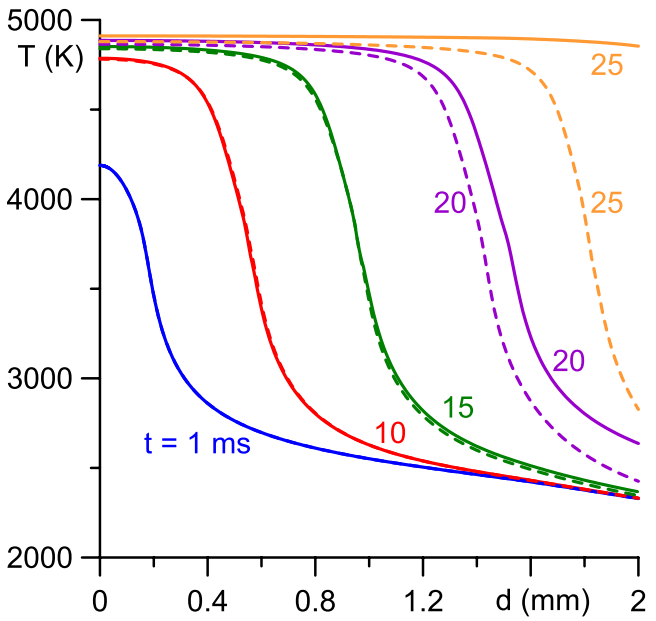

Figure 8. Distributions of the temperature along the cathode surface during the development of a perturbation of a voltage-controlled steady state; dashed: simulations without account of Joule heating; $U = 30$ V, $\beta = 1\%$, $p = 1$ bar, cylindrical cathode with hemispherical tip, $R = 1$ mm, $h = 12$ mm.

4. Stability of current transfer to cathodes of arcs in ambient gas

This section is concerned with the results of the investigation of the stability of stationary solutions describing current transfer to cathodes of arcs in ambient gas. As an example, we will consider conditions of experiments with high-current arcs [21] typical of, e.g., welding devices or plasma torches, and of experiments with low-current arcs [22] typical of HID (high-intensity discharge) lamps. In both cases, the plasma-producing gas is argon. The cathode is made of tungsten and has the shape of a cylinder with hemispherical tip of radius $R = 1$ mm and height $h = 12$ mm under conditions [21] and the shape of a cylinder with a flat front surface with a rounding of radius 100 μm at the edge with $R = 0.75$ mm and $h = 20$ mm under conditions [22]. In both cases, $T_{\rm cool} = 300$ K was set.

Detailed simulations for conditions of experiments [21] and comparison with the experiment have been reported in [6, 23]. Here, we only mention that the current transfer in this case occurs in an axially symmetric mode which embraces states with a hot spot at low currents and states with a diffuse temperature distribution at high currents; a transition between these two regimes occurs with hysteresis. The latter means that graphic representations of characteristics of the mode reveal a retrograde section, which is shown by the dotted line in figure 6.

In principle, the most relevant case for the conditions of experiments [21] is that of a current-controlled spot. Nevertheless, it is of interest to consider also the case of a spot operating at a fixed voltage, for the purposes of comparison with the results for vacuum and also to get an idea of what happens in experiments with high-current arcs in ambient gas if the ballast resistance is not sufficiently high to fix the current.

Voltage-controlled steady states are unstable, similarly to voltage-controlled cathode spots of vacuum arcs. As an example, the temporal evolution of a perturbation of a voltage-controlled steady state with $U = 30$ V (and $I = 6.0$ A) is shown in figures 7 and 8 for the initial perturbation $\beta = 1\%$. d in figure 8 is the distance from the center of the front surface of the cathode measured along the generatrix, so the range $0 \leqslant d \leqslant 1.57$ mm corresponds to the front (spherical) surface of the cathode while the range $d \geqslant 1.57$ mm corresponds to the lateral (cylindrical) surface.

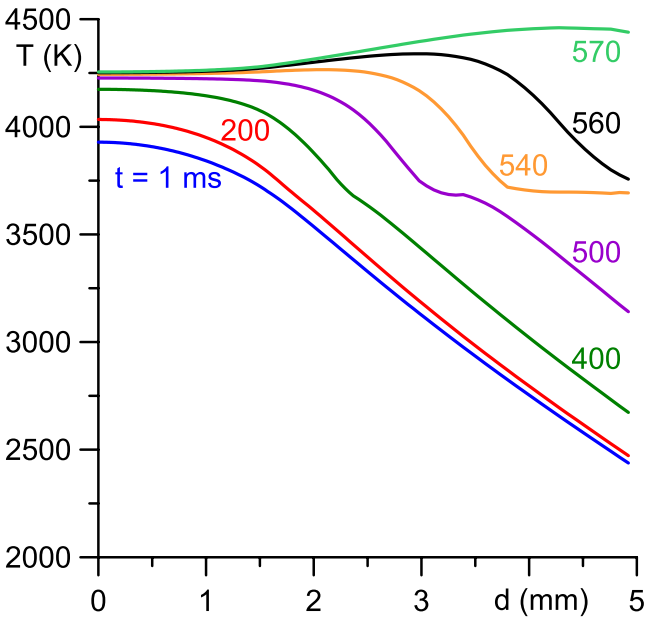

Figure 9. Distributions of the temperature along the cathode surface during the development of a perturbation of a voltage-controlled steady state; $U = 10.2$ V, $\beta = 1\%$, $p = 1$ bar, cylindrical cathode with hemispherical tip, $R = 1$ mm, $h = 12$ mm.

There is no initial decrease in perturbation on the nanosecond scale, in contrast to the case of cathode spots of vacuum arcs, and perturbations develop on the scale of milliseconds. During the first 10 ms the area on the cathode surface heated to temperatures above 4000 K expands from $d \lesssim 0.2$ mm to $d \lesssim 0.6$ mm, the arc current increases from 7 A to approximately 200 A, and $T_{\max}$ increases from 4200 to around 4800 K. In the interval 10 ms $\lesssim t \lesssim$ 25 ms $T_{\max}$ does not change much; however, the area of the hot region and I continue to grow steadily. At around 25 ms the temperature maximum is shifted from the surface into the cathode volume and both $T_{\max}$ and I start growing in an explosive way; however, by that time the whole region $d \lesssim 3$ mm attains a temperature exceeding 4000 K and the arc current exceeds 1 kA. In other words, the whole front surface of the cathode is melted before the explosion could occur. The Joule heating does not significantly affect the massive melting; it would have occurred also in the absence of Joule heating.

As seen from the curve labeled 1 ms in figure 8, the above-considered steady state is associated with a small (of radius around 0.2 mm) spot at the center of the front surface of the cathode, which is typical of the low-current regime. The evolution of perturbations of voltage-controlled steady states with high currents is illustrated in figure 9, which refers to the state with $U = 10.2$ V and $I = 100$ A. There is no spot in this steady state: the whole front surface of the cathode collects current. Again a massive heating occurs, however, on a longer time scale. Note that the maximum of temperature on the lateral surface which is seen for $t \geqslant 540$ ms is due to Joule heating in the cathode body, as discussed in [6], and may be viewed as a precursor of thermal explosion which would have happened a bit later.

Skipping for brevity detailed results for negative perturbations of voltage-controlled steady states, we note that such perturbations result in the destruction of steady states by thermal conduction as in the case of cathode spots of vacuum arcs; however, this happens slower. For example, for $\beta = -1\%$ $T_{\max}$ remains virtually unchanged during an initial interval that varies from $t \approx 1$ ms for $U = 30$ V to 0.3 s for $U = 10.2$ V and then starts decreasing, attaining the value of T_{cool} on the scale of a few seconds.

Current-controlled steady states of current transfer are stable except the intermediate states in the range of hysteresis (i.e. those corresponding to the retrograde section shown by the dotted line in figure 6). These states are unstable: positive thermal perturbations result in a transition to a state belonging to the regime with a diffuse temperature distribution (and a lower $T_{\max}$), and negative perturbations result in a transition to a state belonging to the regime with a hot spot (and a higher $T_{\max}$). It is interesting to note that thermal perturbations change sign in the course of their development in this case.

One can conclude that the pattern of stability of steady states under conditions of high-current arcs in ambient gas has some features in common with the stability of cathode spots in vacuum arcs, but is not quite the same: the instability of voltage-controlled states develops significantly slower and in the case of positive perturbations results in massive melting of the cathode surface rather than in thermal explosion. This difference between arcs in vacuum and ambient gases is indeed observed in the experiment. Intermediate steady states in the range of hysteresis are unstable even if current-controlled.

Let us now consider the conditions of the experiment with low-current arcs [22]. Under these conditions, the current range is narrow and a good control of arc current in the experiment is a must. Therefore, in this work results on stability are reported only for fixed current and perturbations introduced in terms of current variation: the initial condition for the modeling of a steady state corresponding to $I = I_0$ was assumed as the stationary solution corresponding to $I = I_0 + \Delta I$ (it was $\Delta I = \pm 0.1$ A in simulations).

Two modes of current transfer have been observed in the experiment [22], the axially symmetric diffuse mode and a 3D mode with a spot attached at the edge of the front surface of the cathode. Detailed simulations of these two modes and comparison with the experiment have been performed in [22, 24, 25]. Here, we only mention that the diffuse mode exists at all currents and the spot mode exists at $I \lesssim 6.9$ A and comprises two modes (which are usually called branches) separated by a turning point, as shown in figure 10. The spot is hot and well pronounced on the high-voltage branch (the one with a higher voltage in the vicinity of the turning point) and is colder and somewhat diffuse on the low-voltage branch.

Current-controlled steady states of the diffuse mode and the high-voltage branch of the spot mode are stable. Steady states belonging to the low-voltage branch of the spot mode are unstable: development of the perturbation of a steady state with $I = I_0$ results in a steady state with the same current belonging to the diffuse mode or to the high-voltage branch of the spot mode.

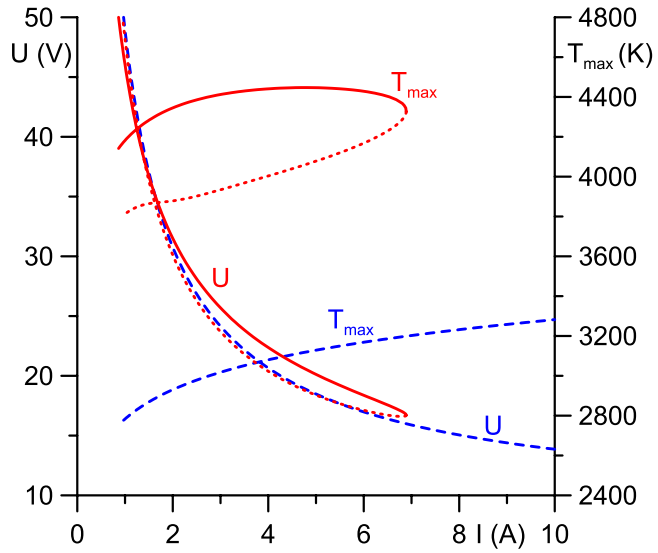

Figure 10. Current–voltage characteristic and maximum temperature of the cathode; solid: high-voltage branch of the spot mode; dotted: low-voltage branch of the spot mode; dashed: diffuse mode; $p = 2.6$ bar, cylindrical cathode with a flat front surface with a rounded edge, $R = 0.75$ mm, $h = 20$ mm.

According to the pattern of stability of the diffuse and spot modes against infinitesimal perturbations [9, 10], the high-voltage branch of the spot mode is stable; the low-voltage branch is unstable; the diffuse mode is stable beyond the first bifurcation point (for $I > I_b$, I_b being the current corresponding to the bifurcation point where the first 3D spot mode branches off from the diffuse mode) and unstable at lower currents (at $I < I_b$). In the experiment [22], the cathode is thin and the first bifurcation point is positioned at very low currents (very high voltages). Therefore, the results on stability against finite perturbations, described in the preceding paragraph, fit into this pattern.

5. Conclusions

Stationary solutions describing steady-state spots on cathodes of vacuum arcs are unstable if the near-cathode voltage is not affected appreciably by ignition or extinction of an individual spot; the case typical of high-power circuit breakers where many tens or even hundreds of spots operate in parallel. Two scenarios of development of the nonlinear phase of instability have been found: thermal explosion for 'positive' thermal perturbations and destruction of the spot by thermal conduction for 'negative' perturbations. The fact that thermal explosion occurs even in the case of planar cathode, which is the one treated in this work, is remarkable, although in this case the time of its beginning is rather long, of the order of 10 μs. Stationary spots are stable if the spot current is not affected by processes in the spot; the case typical of small-scale laboratory experiments.

The stability of stationary regimes of axially symmetric current transfer under conditions of high-current arcs in ambient gas is similar but is not quite the same: the instability of voltage-controlled states develops significantly slower and in the case of positive perturbations results in massive melting of the cathode surface rather than in thermal explosion; current-controlled steady states are stable except the intermediate states in the range of hysteresis.

It follows that if the ballast resistance in a small-scale laboratory experiment with a high-current arc is insufficient, the potential consequence may be thermal explosion of the spot, if the arc burns in vacuum, and massive melting of the cathode surface, if the arc burns in an ambient gas. This conclusion conforms to trends observed in the experiment.

The above-described difference between behaviors of cathode spot in vacuum and ambient gas is a manifestation of the Joule heating being substantial in the case of vacuum and negligible in the case of ambient gas. In order to understand the latter difference, let us compare Q_J the power dissipated in the spot due to Joule effect with Q_c the power loss of a spot due to heat conduction. Q_J is of the order of $j^2 R_s^3/\sigma$ and Q_c of the order of $\kappa T R_s$, R_s being a characteristic value of the spot radius. Thus, the ratio Q_J/Q_c is of the order of $Ij/\kappa\sigma T$. The current per spot and the temperature of spots on copper vacuum arc cathodes and on tungsten cathodes of high-current arcs in ambient gas are comparable. The product $\kappa\sigma$ evaluated at the spot temperature is higher by a factor of about 3 in the case of copper. On the other hand, the current density in the spot on the copper cathode is three orders of magnitude higher than the current density in the case of tungsten cathode; e.g. [26]. Thus, the occurrence of a thermal explosion in the case of copper vacuum cathode and of massive melting in the case of tungsten cathode of arcs in ambient gas is a consequence of very different values of the current density in vacuum and ambient-arc cathode spots.

Note that the dimensionless quantity $Ij/\kappa\sigma T$ has appeared previously in the theory of cathode spots in vacuum arcs: a 1D equation of heat conduction does not admit steady-state solutions if this quantity exceeds a certain value, a result associated with the concept of thermal runaway [27, p 178]. However, the numerical calculations [8] showed that the latter result is irrelevant beyond 1D: a steady-state solution always exists in 2D. In this work, the quantity $Ij/\kappa\sigma T$ has a different meaning: it governs the development of heating instability of voltage-controlled spots.

Current-controlled steady states of the diffuse mode and of the high-voltage branch of the spot mode on a thin cathode typical of low-current arcs in HID lamps are stable. Steady states belonging to the low-voltage branch of the spot mode are unstable. These results fit in the pattern of stability of the diffuse and spot modes against infinitesimal perturbations established previously [9, 10].

Acknowledgments

The work at Universidade da Madeira was supported by FCT— Fundação para a Ciência e a Tecnologia of Portugal through the projects PTDC/FIS-PLA/2708/2012 Modelling, understanding, and controlling self-organization phenomena in plasma-electrode interaction in gas discharges: from first principles to applications and PEst-OE/MAT/UI0219/2014 Centro de Ciências Matemáticas and by Siemens AG.

References

[1] Benilov M S 2008 *J. Phys. D: Appl. Phys.* **41** 144001
[2] Cayla F, Freton P and Gonzalez J-J 2008 *IEEE Trans. Plasma Sci.* **36** 1944
[3] Gonzalez J J, Cayla F, Freton P and Teulet P 2009 *J. Phys. D: Appl. Phys.* **42** 145204
[4] Bergner A, Westermeier M, Ruhrmann C, Awakowicz P and Mentel J 2011 *J. Phys. D: Appl. Phys.* **44** 505203
[5] Baeva M, Kozakov R, Gorchakov S and Uhrlandt D 2012 *Plasma Sources Sci. Technol.* **21** 055027
[6] Benilov M S and Cunha M D 2013 *J. Appl. Phys.* **113** 063301
[7] Baeva M, Uhrlandt D, Benilov M S and Cunha M D 2013 *Plasma Sources Sci. Technol.* **22** 065017
[8] Benilov M S, Cunha M D, Hartmann W, Kosse S, Lawall A and Wenzel N 2013 *IEEE Trans. Plasma Sci.* **41** 1950
[9] Benilov M S 2007 *J. Phys. D: Appl. Phys.* **40** 1376
[10] Benilov M S and Faria M J 2007 *J. Phys. D: Appl. Phys.* **40** 5083
[11] White G K and Minges M L 1997 *Int. J. Thermophys.* **18** 1269
[12] Lewis R W and Ravindran K 2000 *Int. J. Numer. Meth. Eng.* **47** 29
[13] Almeida P G C, Benilov M S and Cunha M D 2008 *J. Phys. D: Appl. Phys.* **41** 144004
[14] Almeida N A, Benilov M S, Benilova L G, Hartmann W and Wenzel N 2013 *IEEE Trans. Plasma Sci.* **41** 1938
[15] Benilov M S, Cunha M D and Naidis G V 2005 *Plasma Sources Sci. Technol.* **14** 517
[16] Almeida P G C, Benilov M S, Cunha M D and Gomes J G L 2013 *Plasma Sources Sci. Technol.* **22** 012002
[17] Beilis I I 2013 *IEEE Trans. Plasma Sci.* **41** 1979
[18] Hantzsche E 1983 *IEEE Trans. Plasma Sci.* **11** 115
[19] Hantzsche E 2003 *IEEE Trans. Plasma Sci.* **31** 799
[20] Beilis I I 2010 *Appl. Phys. Lett.* **97** 121501
[21] Mitrofanov N K and Shkol'nik S M 2007 *Tech. Phys.* **52** 711
[22] Dabringhausen L, Langenscheidt O, Lichtenberg S, Redwitz M and Mentel J 2005 *J. Phys. D: Appl. Phys.* **38** 3128
[23] Benilov M S, Cunha M D and Faria M J 2009 *J. Phys. D: Appl. Phys.* **42** 145205
[24] Benilov M S, Carpaij M and Cunha M D 2006 *J. Phys. D: Appl. Phys.* **39** 2124
[25] Scharf F H, Langenscheidt O and Mentel J 2007 *Proc. 28th ICPIG (Prague, Czech Republic, July 2007)* ed J Schmidt *et al* (Prague: Institute of Plasma Physics AS CR) pp 1252-5 ISBN 978-80-87026-01-4
[26] Benilov M S and Benilova L G 2013 *J. Appl. Phys.* **114** 063307
[27] Hantzsche E 1995 *Handbook of Vacuum Arc Science and Technology: Fundamentals and Applications* ed R L Boxman *et al* (Park Ridge, NJ: Noyes Publications) pp 151–208